Optoelectronic properties of hexagonal boron nitride epilayers

X. K. Cao, S. Majety, J. Li, J. Y. Lin* and H. X. Jiang*

Department of Electrical and Computer Engineering, Texas Tech University, Lubbock, TX 79409

ABSTRACT

This paper summarizes recent progress primarily achieved in authors' laboratory on synthesizing hexagonal boron nitride (hBN) epilayers by metal organic chemical vapor deposition (MCVD) and studies of their structural and optoelectronic properties. The structural and optical properties of hBN epilayers have been characterized by x-ray diffraction (XRD) and photoluminescence (PL) studies and compared to the better understood wurtzite AlN epilayers with a comparable energy bandgap. These MOCVD grown hBN epilayers exhibit highly efficient band-edge PL emission lines centered at around 5.5 eV at room temperature. The band-edge emission of hBN is two orders of magnitude higher than that of high quality AlN epilayers. Polarization-resolved PL spectroscopy revealed that hBN epilayers are predominantly a surface emission material, in which the band-edge emission with electric field perpendicular to the c-axis ($E_{emi}\perp c$) is about 1.7 times stronger than the component along the c-axis ($E_{emi}//$c). This is in contrast to AlN, in which the band-edge emission is known to be polarized along the c-axis, ($E_{emi}//$c). Based on the graphene optical absorption concept, the estimated band-edge absorption coefficient of hBN is about 7×10^5 cm^{-1}, which is more than 3 times higher than the value for AlN ($\sim2\times10^5$ cm^{-1}). The hBN epilayer based photodetectors exhibit a sharp cut-off wavelength around 230 nm, which coincides with the band-edge PL emission peak and virtually no responses in the long wavelengths. The dielectric strength of hBN epilayers exceeds that of AlN and is greater than 4.5 MV/cm based on the measured result for an hBN epilayer released from the host sapphire substrate.

Key words: Hexagonal boron nitride, wide bandgap semiconductors, deep UV photonics

1. INTRODUCTION

Hexagonal boron nitride (hBN) possesses amazing physical properties including high temperature stability and corrosion resistance, large optical absorption and neutron capture cross section, and relative large negative electron affinit.[1-4] Among the members of the III-nitride material system, boron nitride having a band gap comparable to AlN ($E_g \sim 6$ eV), is the least studied and understood. Due to its layered structure and similar lattice constants to graphene, hBN is also considered as the ideal template and gate dielectric layer in graphene electronics and optoelectronics.[5-9]

Due to its high bandgap and in-plane thermal conductivity, hBN has been considered both as an excellent electrical insulator and thermal conductor. However, lasing action in deep ultraviolet (DUV) region (~225 nm) by electron beam excitation was demonstrated in small hBN bulk crystals synthesized by a high pressure/temperature technique,[10] raising its promise as a semiconducting material for realizing chip-scale DUV light sources/sensors. So far, hBN bulk crystals with size up to millimeters can be grown. Other than small size, bulk crystal growth has disadvantages of difficulty to control growth conditions such as intentional doping and formation of quantum well based device structures and is more suitable for synthesizing bulk crystals as substrates if single crystal growth techniques can be scaled to produce large wafers. The synthesis of wafer-scale semiconducting hBN epitaxial layers with high crystalline quality and electrical conductivity control is highly desirable for the fundamental understanding and the exploration of emerging applications of this interesting material. This paper summarizes recent progress primarily achieved

in authors' laboratory on synthesizing hBN epilayers by MOCVD and studies of their structural and optoelectronic properties.[4,11-14] Detailed comparison studies with high quality and well characterized AlN epilayers have been carried out.[15-19]

2. EXPERIMENT

Hexagonal BN epitaxial layers were synthesized by metal organic chemical vapor deposition (MOCVD) using triethylboron (TEB) source and ammonia (NH_3) as B and N precursors, respectively. Prior to epilayer growth, a 20 nm BN buffer layer was first deposited on sapphire substrate at 800 ^{o}C. The typical hBN epilayer growth temperature was about 1300 ^{o}C using hydrogen as a carrier gas with a growth rate of 0.5 μm/hr. AlN epilayers were grown by MOCVD on sapphire substrates. The sources of Al and N are Trimethylaluminium (TMAl) and blue ammonia, respectively. X-ray diffraction (XRD) was employed to determine the lattice constant and crystalline quality of the epilayers. The PL spectroscopy system consists of a frequency quadrupled 100 femtosecond Ti: sapphire laser with excitation photon energy set around 6.28 eV and a monochromator (1.3 m). A single photon counting detection system together with a micro-channel-plate photo-multiplier tube was used to record PL spectra. The fabrication procedures for hBN and AlN DUV metal-semiconductor-metal (MSM) photodetectors consisted of the following steps.[14,18,19] First, photolithography was employed to define the micro-scale strips (5 μm/5 μm width/spacing). A bilayer of 5 nm/5 nm (Ni/Au) was deposited using e-beam evaporation to form the Schottky contacts for hBN and a Pt (10 nm) layer was deposited using e-beam evaporation to form the Schottky contacts on AlN. Bonding pads were then formed by depositing an Au (200 nm) layer. Finally, the sapphire substrates were polished and thinned to about 100 μm and diced to discrete devices, which were bonded onto device holders for characterization. The system for the spectral responses and I-V characteristics measurements consists of a deuterium light source, monochromator, source-meter, and electrometer. The light source was dispersed by the monochromator to obtain excitation photons with different wavelengths.
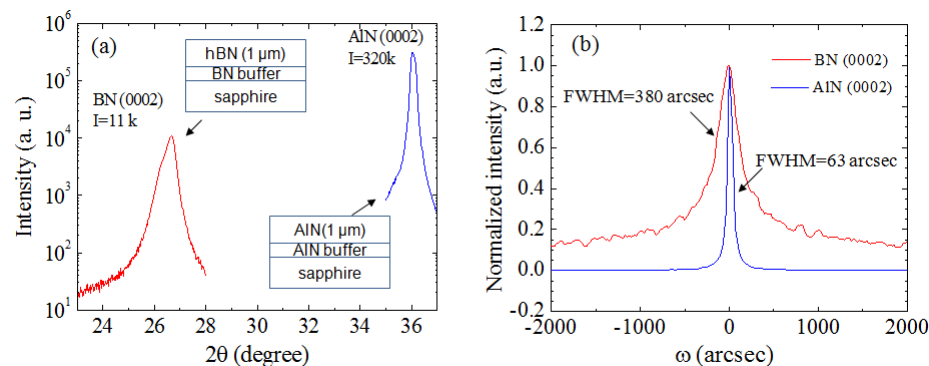
3. RESULTS AND DISCUSSION

Fig. 1 Comparison XRD results of hBN and AlN epilayers: (a) θ-2θ scan[14] and (b) rocking curve of the (0002) reflection peaks.

Figure 1 compares XRD characterization results for AlN and hBN. θ-2θ scan for an hBN epilayer of 1 μm in thickness shown in Fig. 1(a) revealed a *c*-lattice constant ~6.67 Å, which closely matches to the bulk *c*-lattice constant of hBN (c=6.66 Å),[1,20] affirming that BN films are of single hexagonal phase. However, the XRD intensity of the (0002) peak of hBN is about 30 times lower than that of AlN epilayer with the same thickness.[14] As shown in Fig. 1(b), the XRD rocking curve of the (0002) diffraction peak has a

full width at half maximum (FWHM) of ~380 arcsec for the hBN,[11] which is a dramatic improvement over previously reported values for hBN films (1.5^0-0.7^0),[21] but is much broader than the typical FWHM of high quality AlN epilayers of <100 arcsec.[17] The results are an indicative of the fact that the development of epitaxial layers of hBN is in its early stage.
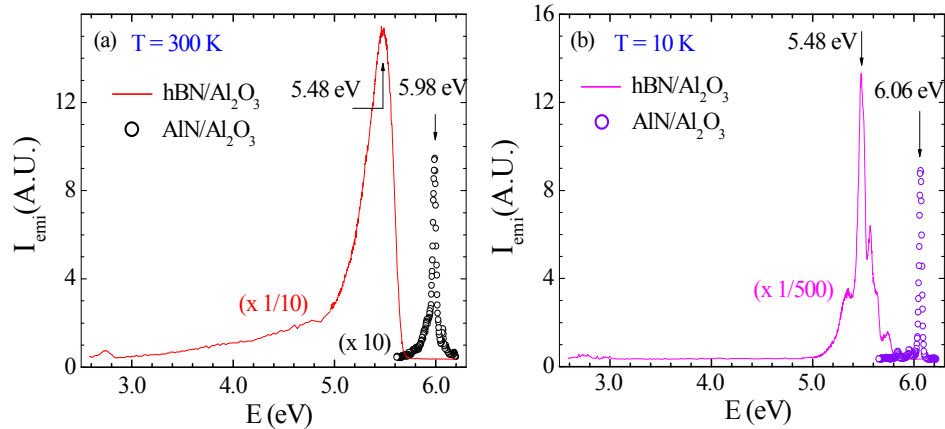

Fig. 2 Comparison DUV PL spectra of hBN and AlN epilayers measured at (a) 10 K and (b) 300 K.[13]

As with other semiconductor materials in their early development stages, realizing the band-edge PL emission at room temperature is a *prerequisite* in research and *development* towards practical applications of hBN. Figure 2 shows the comparison of PL spectra of our hBN and AlN epilayers measured side-by-side at (a) 10 K and (b) 300 K.[13] A strong band-edge PL emission centered at about 5.48 eV at 10 K was observed in hBN. We notice that the spectral peak position of the free exciton emission line in AlN exhibits a red-shift with increasing temperature, following the bandgap variation with temperature of AlN.[15] For hBN, we are unable to detect the variation of the spectral peak position with temperature. Furthermore, the band-edge PL emissions from hBN at low and room temperatures are more than two orders of magnitude higher than that of AlN, which is considered to be a highly efficient emission material and is the current default choice for DUV device implementation. One of the major reasons for the high band-edge emission efficiency in hBN is thought to be due to its layered structure.[22] Recent theoretical studies have also suggested that an efficient band-edge emission is expected from hBN due to its graphite like layered structure and small lattice constant in the c-plane.[23, 24] The layer structured hBN provides a natural 2D system which can result in an increase in the exciton binding energy and oscillator strength over the 3D systems such as AlN.[25] Another factor that may account for this efficient band-edge emission in hBN is the high band-edge optical absorption coefficient.[3]

The previously measured band-edge optical absorption coefficient (α) of hBN is unusually high (~ 7.5 x 10^5 cm^{-1}) and is more than 3 times higher than that of AlN (~ 2x10^5 cm^{-1}).[3, 26, 27] To understand this unique property, we write the optical absorption (I) as[14]

$$I=I_0 (1-e^{-t/\lambda}); \tag{1}$$

where λ is the optical absorption length. On the other hand, we can rewrite Eq. (1) as follows,

$$I/I_0 \approx (t/\lambda), \text{ for } (t/\lambda) <<1; \tag{2}$$

One important and interesting features of graphene is that its absorption is determined by fundamental constants following $\pi e^2/\hbar c=\pi\alpha=2.3\%$ where $\alpha=e^2/\hbar c$ is the fine structure constant, which describes the coupling between light and relativistic electrons.[28] If we assume the same holds for hBN, we then have the

optical absorption of hBN = 2.3% per layer (3.33 Å). This means that $I/I_0 = (t/\lambda) = 0.023$ with t=3.33 Å. This gives,

$$\lambda = t/0.023 = 3.33 \text{ Å}/0.023 = 144.8 \text{ Å}$$
$$\alpha = 1/\lambda = 1/144.8 \text{ Å} = 6.9 \times 10^{-3}/\text{Å} \approx 7 \times 10^5/\text{cm}.$$

The estimated value of the band-edge optical absorption coefficient (α) based on the optical absorption concept from graphene agrees exceptionally well with the previously measured value of about 7.5 $\times 10^5$/cm.[3] This means that only a very thin layer of hBN with approximately 70 nm (~5λ) in thickness will absorb all incoming above bandgap photons. This together with its inherent nature of layered structure makes hBN an exceptionally efficient emitter.
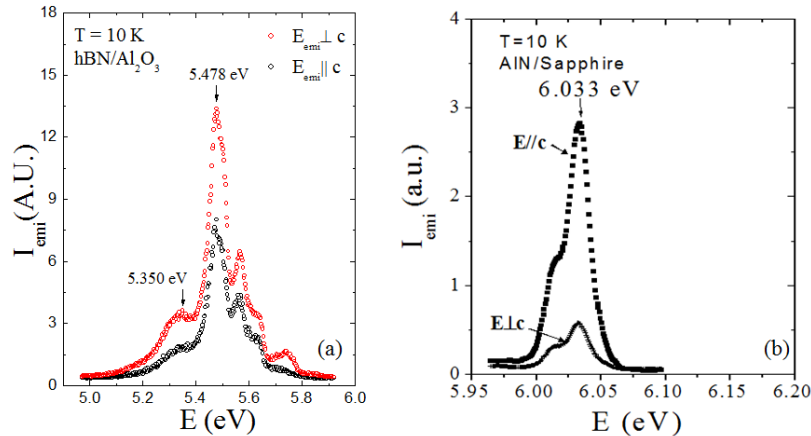

Fig. 3 Low temperature (10 K) polarization-resolved band-edge PL spectra of (a) hBN and (b) AlN epilayer with emission polarization parallel ($E_{emi}//c$) and perpendicular ($E_{emi}\perp c$) to the c-axis. Excitation laser line is polarized in the direction perpendicular to the c-axis ($E_{emi}//c$).[13, 16]

Figure 3 compares the polarization-resolved band-edge PL emission spectra of hBN and AlN epilayers measured at 10K.[13,16] The PL emission spectral line shape for hBN shown in Fig. 3(a) for the configuration with emission polarization along the crystal c-axis ($E_{emi}//c$) is observed to be very similar to that in the ($E_{emi}\perp c$) configuration. However, we have noticed that the emission intensity is about 1.7 times stronger in ($E_{emi}\perp c$) configuration, which is similar to some of the well understood semiconductor materials including GaN;[29] however, is in sharp contrast to the polarization-resolved PL spectra of AlN shown in Fig. 3(b).[16] It is now a well established fact that the band-edge emission in AlN is polarized along the c-axis, ($E_{emi}//c$), due to the nature of its band structure (the negative crystal-field splitting in AlN).[16,30] This polarization property of AlN has a profound impact on the device applications. For instance, for UV light emitting diodes (LEDs) using c-plane Al-rich $Al_xGa_{1-x}N$ as active layers, the most dominant emission will be polarized along the c-axis ($E_{emi}//c$), which implies that UV photons can no longer be extracted easily from the surface.[30] Thus, incorporating methods for enhancing the light extraction is critical in AlGaN UV LEDs.[31] Furthermore, in contrast to all conventional semiconductor laser diodes with lasing output polarized in the transverse-electric field (TE) mode, it was predicated[30] and experimentally verified[32] that lasing radiation from c-plane Al-rich $Al_xGa_{1-x}N$ based laser diodes is strongly polarized in the transverse-magnetic-field (TM) mode. These are currently critical issues facing the development of deep UV light emitting devices based on AlGaN. Thus, the observed predominant ($E_{emi}\perp c$) polarization of the band-edge emission in hBN is an advantageous feature over AlN for UV light emitting device applications.

The relative spectral responses of hBN and AlN MSM photodetectors have been measured at different bias voltages and examples are shown in Fig. 4.[14, 18] The hBN MSM photodetectors exhibit a peak responsivity of 220 nm, a sharp cut-off wavelength around 230 nm, which corresponds well with the band-edge

PL emission peak at 5.48 eV (or 227 nm).[14] The AlN MSM photodetectors exhibit a peak responsity of 200 nm, an extremely sharp cut-off wavelength around 207 nm.[18] An outstanding feature observed from hBN photodectors is that there are virtually no detectable responses in the long wavelengths measured up to 800 nm. Figure 5 compares the I-V characteristics of MSM photodetectors based on hBN and AlN epilayers. The dark current density in AlN photodetectors is around of $\sim 10^{-9}$ A/cm^2 at a bias voltage of 100 V. Similar to AlN devices, hBN devices exhibit rather low dark current density of $\sim 10^{-10}$ A/cm^2 at a bias voltage of 100 V, the observed DUV to visible rejection ratio in hBN MSM detectors is still 2-3 orders of magnitude lower than that of AlN based detectors.[14,18,19] This corroborates the fact that the crystalline quality of hBN epilayers is not yet as good as those of high quality AlN epilayers, as confirmed by the XRD results shown in Fig. 1.
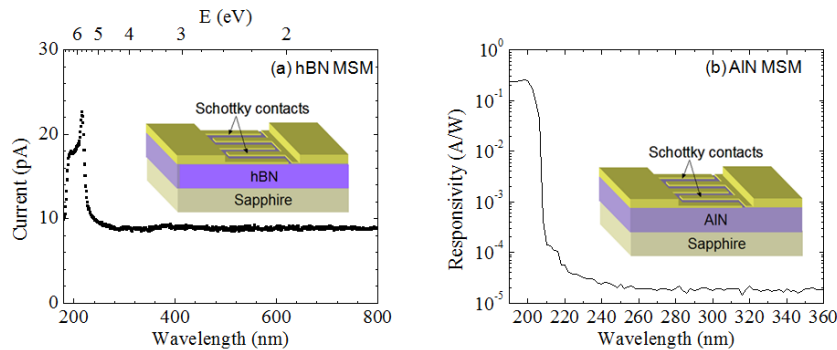

Fig. 4 The relative spectral responses of (a) hBN and (b) AlN MSM photodetectors measured at a bias of 30 V. The insets shows the material layer structures utilized for the fabrication of photodetectors. The hBN devices have a cross-section area of 1.25 mm x 0.8 mm and AlN devices have a cross-section area of 80 μm x 80 μm.
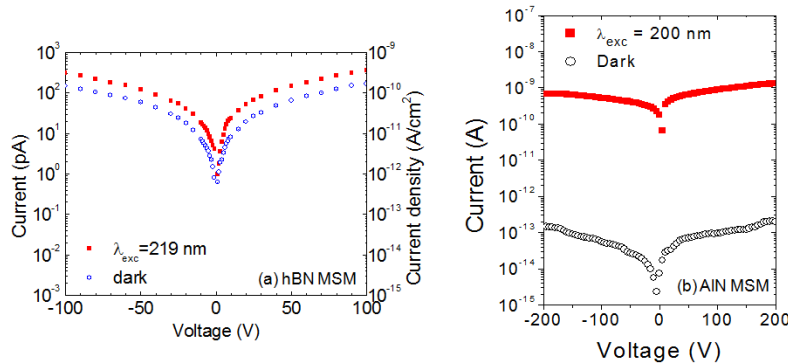

Fig. 5 I-V characteristic of MSM photodetector based on (a) hBN and (b) AlN epilayers.

One other important parameter of a semiconductor for detector applications is the dielectric strength or the breakdown field (E_B) in the c-direction. A previous study has obtained E_B=7.94 MV/cm for ultrathin hBN layers mechanically exfoliated from powder crystals.[33] Since our hBN epilayers were grown on sapphire substrates, it was necessary to released epilayers from the host sapphire substrate in order to conduct E_B measurements. We first deposited a bilayer of Ni/Au Schottky contact on a 1.8 μm thick hBN epilayer and then coated the Ni/Au Schottky contact with Ag past. Next, we glued the structure to a second sapphire substrate and then released the epilayer from the host sapphire substrate by mechanical force. Finally, another bilayer of Ni/Au Schottky contact was deposited on the back side of the released hBN epilayer. A schematic of the device structure for E_B measurements is shown in the inset of Fig. 6. Figure 6 shows the I-V characteristics of the released hBN epilayer in the c-direction (out-of-plane), which indicate that the breakdown occurs at around 810 V. This translates to $E_B \sim 4.5$ MV/cm, which is lower than that obtained

from ultrathin hBN layers exfoliated from powder crystals having a cross section area in micron scale.[33] Not only our released hBN epilayer used for E_B measurement has a large cross section area of ~4 mm^2, but hBN epitaxial layers are grown on foreign substrate and are not dislocation free. Moreover, the backside of the released hBN epilayer contains a 20 nm low temperature buffer layer of amorphous nature, which also reduced the measured value of E_B of hBN.
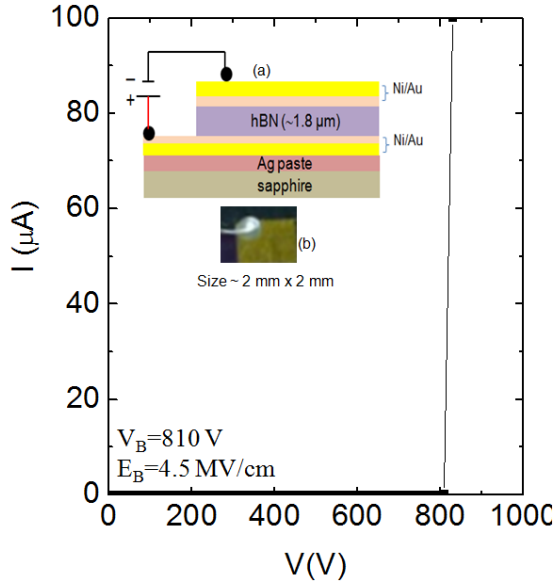

Fig. 6 Out-of-plane (vertical) I-V characteristics of a released hBN epilayer, which has a cross section area of about ~4 mm^2. Inset (a) is the schematic of an hBN epilayer released from the host sapphire substrate and (b) the microscope image of the device employed for breakdown field measurement.[14]
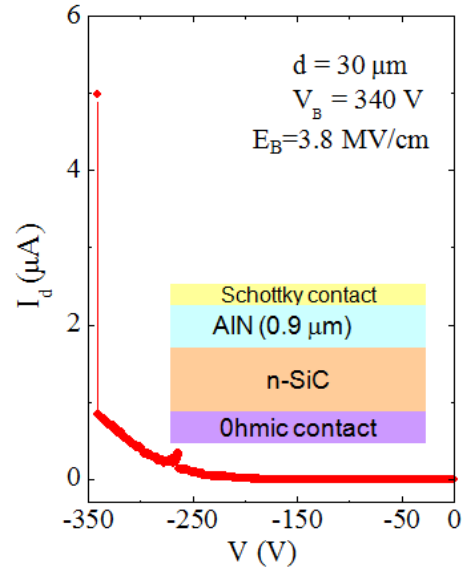
Fig. 7 Reverse bias I-V characteristics of AlN Schottky detector with d = 30 μm in diameter. The measured breakdown voltage, V_B, is around 340 V. Inset shows the schematic of the AlN/n-SiC Schottky detector layer structure employed for breakdown field measurement.[19]

The breakdown field of AlN epilayers in the *c*-direction (out-of-plane) has been previously measured via a vertical Schottky detector structure of AlN grown on n-type SiC (AlN/n-SiC),[19] as illustrated schematically in the inset of Fig. 7. The I-V characteristic of an AlN/n-SiC Schottky detector with a 30 μm in diameter is shown in Fig. 7, which shows that the AlN device exhibits a breakdown voltage of about 340 V and a breakdown field of about 3.8 MV/cm. It was further demonstrated that E_B increases linearly with a decrease in the device area (A), since the number of dislocations decreases linearly with a decrease in A.[19] E_B for dislocation-free AlN epilayers can be obtained by extrapolating A to zero (~4.1 MV/cm).[19] Our results shown in Fig. 6 and 7 clearly indicate that hBN epilayers have a higher E_B than AlN epilayers. If we assume ultrathin hBN layers exfoliated from powder crystals are dislocation free,[33] then the value of 7.94 MV/cm may represent the E_B value of intrinsic hBN. Our results thus suggest that the device performance can be improved by improving material quality, mainly reducing dislocation density, and optimizing the device size and geometry.

4. SUMMARY

Significant progress in MOCVD growth of hBN epilayers has been made. The band edge emission in hBN is very efficient and is more than two orders of magnitude higher than that in AlN epilayers. Polarization-resolved PL results have revealed that hBN is predominantly a surface emission material with

light output polarized in the TE mode. Based on the graphene optical absorption concept, the estimated band-edge absorption coefficient of hBN is about 7×10^5/cm, which is more than 3 times higher than the value for AlN ($\sim2\times10^5$ /cm). The dielectric strength of hBN epilayers exceeds that of AlN epilayers and is greater than 4.4 MV/cm based on the measured result for an hBN epilayer released from the host sapphire substrate. Thus, hBN is a material with a very low dielectric constant, but having a very high dielectric strength. The hBN epilayer based DUV detectors have a sharp cut-off wavelength around 230 nm, which coincides with the band-edge PL emission peak and showed virtually no response in the long wavelengths measured up to 800 nm. Currently, our understanding of hBN epilayer growth and properties is still in the very early stage compared to the status of AlN epilayers. Much improvement is anticipated for hBN, which ultimately will lead to functional practical devices. However, our results indicate that device quality hBN epilayers can be produced by MOCVD technique. The present results together with the ability of p-type doping of hBN[34] represents a major step towards the realization of hBN based practical devices.

ACKNOWLEDGEMENTS

REFERENCES

a) hx.jiang@ttu.edu; jingyu.lin@ttu.edu

[1] S. L. Rumyantsev, M. E. Levinshtein, A. D. Jackson, S. N. Mohammmad, G. L. Harris, M. G. Spencer, and M. S. Shur, in *Properties of Advanced Semiconductor Materials GaN, AlN, InN, BN, SiC, SiGe* . edited by M. E. Levinshtein, S. L. Rumyantsev, and M. S. Shur (John Wiley & Sons, Inc., New York, 2001), p. 67-92.

[2] Y. Kubota, K. Watanabe, O. Tsuda and T. Taniguchi, Science **317**, 932 (2007).

[3] T. Sugino, K. Tanioka, S. Kawasaki, and J. Shirafuji, Jpn. Appl. Phys. **36**, L463 (1997).

[4] J. Li, R. Dahal, S. Majety, J.Y. Lin, and H.X. Jiang, Nuclear Instruments and Methods in Physics Research A, **654**, 417, (2011).

[5] L. Song, L. Ci, H. Lu, P. B. Sorokin, C. Jin, J. Ni, A.G. Kvashnin, D. G. Kvashnin, J. Lou, B. I. Yakobson, and P. M. Ajayan, Nano. Lett. **10**, 3209 (2010).

[6] R. V. Gorbachev, I. Riaz , R. R. Nair, R. Jalil, L. Britnell, B. D. Belle, E. W. Hill, K. S. Novoselov, K. Watanabe, T. Taniguchi, A. K. Geim, and P. Blake, Small, **7**, 465 (2011).

[7] Y. Shi, C. Hamsen, X. Jia, K. K. Kim, A. Reina, M. Hofmann, A. L. Hsu , K. Zhang, H. Li, Z. Y. Juang, M. S. Dresselhaus, L. J. Li, and J. Kong, Nano Lett. **10**, 4134 (2010).

[8] N. Alem, R. Erni, C. Kisielowski, M. D. Rossell, W. Gannett, and A. Zettl, Phys. Rev. B **80**, 155425 (2009).

[9] C. R. Dean, A. F. Young, I. Meric, C. Lee, L. Wang, S. Sorgenfrei, K. Watanabe, T. Taniguchi, P. Kim, K. L. Shepard and J. Hone, Nature Nanotechnology **5**, 722 (2010).

[10] K. Watanabe, T. Taniguchi, and H. Kanda, Nature Materials, **3**, 404 (2004).

[11] R. Dahal, J. Li, S. Majety, B. N. Pantha, X. K. Cao, J. Y. Lin, and H. X. Jiang, Appl. Phys. Lett., **98**, 211110, (2011).

[12] S. Majety, J. Li, X. K. Cao, R. Dahal, B. N. Pantha, J. Y. Lin, and H. X. Jiang, Appl. Phys. Lett. **100**, 061121 (2012).

[13] S. Majety, X. K. Cao, J. Li, R. Dahal, J. Y. Lin and H. X. Jiang, Appl. Phys. Lett. **101**, 051110 (2012).

[14] J. Li, S. Majety, R. Dahal, W. P. Zhao, J. Y. Lin, and H. X. Jiang, Appl. Phys. Lett. **101**, 171112 (2012).

[15] K. B. Nam, J. Li, M. L. Nakarmi, J. Y. Lin and H. X. Jiang, Appl. Phys. Lett. **82**, 1694 (2003).

[16] J. Li, K. B. Nam, M. L. Nakarmi, J. Y. Lin, and H. X. Jiang, P. Carrier, and S.-H. Wei, Appl. Phys. Lett. **83**, 5163 (2003).

[17] B. N. Pantha, R. Dahal, M. L. Nakarmi, N. Nepal, J. Li, J. Y. Lin, H. X. Jiang, Q. S. Paduano, and D. Weyburne, Appl. Phys. Lett. **90**, 241101 (2007).

[18] J. Li, Z. Y. Fan, R. Dahal, M. L Nakarmi, J. Y. Lin, and H. X. Jiang, Appl. Phys. Lett. **89**, 213510 (2006).

[19] R. Dahal, T. M. Al Tahtamouni, J. Y. Lin, and H. X. Jiang , Appl. Phys. Lett. **91**, 243503 (2007).

[20] R. S. Pease, Acta.Cryst., **5**, 356 (1952).

[21] Y. Kobayashi, T. Akasaka, and T. Makimoto J. Crystal Growth **310**, 5048 (2008).

[22] B. Huang, H. X. Jiang, X. K. Cao, J. Y. Lin, and Su-Huai Wei, Phys. Rev. B. **86**, 155202 (2012).

[23] L. Museur, G. Brasse, A. Pierret, S. Maine, B. Attal-Trétout, F. Ducastelle, A. Loiseau, J. Barjon, K. Watanabe, T. Taniguch, and A. Kanaev, Phys. Status Solidi RRL **5**, 214 (2011).

[24] B. Arnaud, S. Lebègue, P. Rabiller, and M. Alouani, Phys. Rev. Lett. **96**, 026402 (2006).

[25] P. K. Basu, Theory of Optical Processes in Semiconductors: Bulk and Microstructures (Clarendon Press, Oxford 1997).

[26] P. B. Perry and R. F. Rutz, Appl. Phys. Lett. **33,** 319 (1978).

[27] H. Demiryont, L. R. Thompson, and G. J. Collins, Appl. Optics **25**, 1311 (1986).

[28] R. R. Nair, P. Blake, A. N. Grigorenko, K. S. Novoselov, T. J. Booth, T. Stauber, N. M. R. Peres, and A. K. Geim, Science, **320** 1308 (2008).

[29] G. D. Chen, M. Smith, J. Y. Lin, H. X. Jiang, S.-H. Wei, M. Asif Khan, and C. J. Sun, Appl. Phys. Lett. **68**, 2784 (1996).

[30] K. B. Nam, J. Li, M. L. Nakarmi, J. Y. Lin, and H. X. Jiang, Appl. Phys. Lett. 84, 5264 (2004).

[31] J. Shakya, K. H. Kim, J. Y. Lin, and H. X. Jiang, Appl. Phys. Lett. **85**, 142 (2004).

[32] H. Kawanishi, M. Senuma, and T. Nukui, Appl. Phys. Lett. **89**, 041126 (2006).

[33] G. H. Lee, Y. J. Yu, C. Lee, C. Dean, K. L. Shepard, P. Kim, and J. Hone, Appl. Phys. Lett. **99**, 243114 (2011).

[34] R. Dahal, J. Li, S. Majety, B. N. Pantha, X. K. Cao, J. Y. Lin, and H. X. Jiang, Appl. Phys. Lett. **98**, 211110 (2011).